



Computed Tomography Imaging of Cavum nasi and Sinus paranasales in the Tuj Sheep

Yasin DEMIRASLAN^{1,a}, Mustafa Orhun DAYAN^{2,b}, Kemal ERTILAV^{3,c}, Yalçın AKBULUT^{4,d}, Sema ÖZKADIF^{5,e}, Özcan ÖZGEL^{1,f}

¹ Department of Anatomy, Faculty of Veterinary Medicine, Burdur Mehmet Akif Ersoy University, Burdur, Turkey

² Department of Anatomy, Faculty of Veterinary Medicine, Selcuk University, Konya, Turkey

³ Isparta Vocaitonal School of Health Services, Suleyman Demirel University, Isparta; Turkey

⁴ Department of Anatomy, Faculty of Medicine, Kars Kafkas University, Kars, Turkey

⁵ Department of Anatomy, Faculty of Veterinary Medicine, Cukurova University, Adana, Turkey

^aORCID: 0000-0003-3612-6142; ^bORCID: 0000-0003-0368-4607; ^cORCID: 0000-0002-0520-0672

^dORCID: 0000-0003-4661-2224; ^eORCID: 0000-0002-5398-9874; ^fORCID: 0000-0003-0394-5678

Geliş Tarihi/Received
20.09.2019

Kabul Tarihi/Accepted
28.02.2020

Yayın Tarihi/Published
30.06.2020

Abstract

The aim of this study was to scan cavum nasi and sinus paranasales in male Tuj sheep with computed tomography. Skulls of 8 adult male Tuj sheep were used for the study. On the skulls that computed tomography images were received, cavum nasi and relevant anatomic structures were discerned through 2-dimensional images. Surface area and volume of sinus paranasales were determined through 3-dimensional images. Sinus maxillaris was found to extend from the level of mesial cusp of 2nd maxillary premolar tooth to the lateral angle of the eye. Sinus frontalis was found to extend from the interproximal level between the 3rd maxillary premolar and the 1st maxillary molar to the horn base. Total volume and surface area of sinus paranasales in the skulls of Tuj male sheep on the average were found to be 76963,89 mm³, 39595,96 mm² respectively. The sinuses with the largest and smallest volume were sinus frontalis and sinus lacrimalis, respectively. In conclusion, it is considered that the information and the data obtained in this study will enable researchers to make radiological assessments on cavum nasi and paranasal sinus in Tuj sheep and compare them with other sheep breeds.

Key Words: Computed tomography, nasal cavity, paranasal sinuses, sheep

Tuj Koyununda Cavum nasi ve Sinus paranasales'in Bilgisayarlı Tomografi İle Görüntülenmesi

Öz

Çalışmada erkek Tuj koyununda cavum nasi ve sinus paranasales'in bilgisayarlı tomografi ile görüntülenmesi amaçlanmıştır. Çalışma için 8 adet erişkin erkek Tuj koyunu başı kullanıldı. Bilgisayarlı tomografi görüntüleri alınan başlarda 2 boyutlu görüntüler üzerinden cavum nasi ve ilgili anatomik yapılar ayırt edildi. 3 boyutlu görüntüler üzerinden sinus paranasales yüzey alanı ve hacmi belirlendi. Sinus maxillaris'in 2. maxillar premolar dişin ön ucu seviyesinden başlayıp lateral göz açısı seviyesine kadar uzandığı tespit edildi. Sinus frontalis'in 3. maxillar premolar ve 1. maxillar molar dişler arası seviyesinden başlayıp boynuz kaidesine kadar uzandığı belirlendi. Tuj koyunu başlarında toplam sinus paranasales hacminin ve yüzey alanının sırasıyla ortalama 76963,89 mm³, 39595,96 mm² olduğu görüldü. En büyük ve en küçük hacme sahip sinus lar sırasıyla sinus frontalis ve sinus lacrimalis'ti. Sonuç olarak bu çalışmada elde edilen bilgilerin ve verilerin Tuj koyununda cavum nasi ve paranasal sinus'lerin radyolojik değerlendirmelerine, ayrıca diğer koyun ırkları ile karşılaştırılmalarına olanak sağlayacağı düşünülmektedir.

Anahtar Kelimeler: Bilgisayarlı tomografi, burun boşluğu, paranasal sinus, koyun

INTRODUCTION

Tuj sheep breeding in North East Anatolia Region belongs to potential of 0.03 % in among the sheep races found in Turkey. Tuj sheep is known as Tuchin in Caucasia Region (1,2).

Conchas (dorsal, median, and ventral) and meatuses between those in cavum nasi in ruminantia are the anatomically first notable structures. Sinus paranasales in ruminantia is composed of sinus conchae dorsalis, sinus conchae medius, sinus palatinus, sinus lacrimalis, sinus frontalis and sinus maxillaris (3). Clinically, comprehending the positions,

extension, and connections with cavum nasi and other structures of paranasal sinuses is important to interpret upper respiratory tract infections (4-6). In addition, cavum nasi and sinus paranasales present clinical symptoms in infective, non-infective, traumatic, dental or nasopharyngeal diseases (6,7). Computed tomography (CT) is an alternative imaging method which enables the exploration of structures in the skull region thanks to scanning radiography (8). There are researches (9-11) on computed tomography and examinations of anatomic structures of sinus paranasales and cavum nasi related to different breeds in ruminantia in the literature. In this study, we aimed to scan

cavum nasi and sinus paranasales with computed tomography in Tuj sheep and describe the anatomical structures there for the use of veterinary anatomists, students, researchers, and veterinary clinicians.

MATERIALS AND METHODS

Skulls of 8 adult Tuj male sheep were used for the study. Average body weight of the sheep was 65 kg (SD: 5.6 kg) and they were clinically healthy animals. The skulls were supplied from the slaughterhouse and butchers of Kars province. First 0.9% saline water and then 10% formaldehyde were injected to the heads before arteria carotis communis. Following the formaldehyde injection two heads were kept frozen for the subsequent CT imaging and cross-sectional anatomy. The CT images of the heads were obtained in Kafkas University Training and Research Hospital Radiology Unit (Scan Parameters: 120 kV, 250 mA) in 48 hours. Cavum nasi, sinus paranasales, and related anatomical structures were discerned through the 2-dimensional images. The surface area and the volume of sinus paranasales were determined through the 3-dimensional images (MIMICS 13.0 Software) (Figure 1, 2). The mean and standard deviation values of all the measurements obtained were analysed by using Statistical Package for the Social Sciences programme. In terminology, Nomina Anatomica Veterinaria (12) was used.

RESULTS

Cavum nasi (meatus nasales, concha nasals), the bone tissue surrounding it, and the structures connected with the Sinus paranasales were discerned at an impressive level in the 2-dimensional images that were obtained by CT in the study. The details on 2-dimensional CT images were shown in Figure 3, 5, 7, 9, 11. Furthermore, the structures of cross-sectional section of Tuj sheep's head were shown in Figure 4, 6, 8, 10, 12. Sinus paranasales in Tuj sheep were found to be sinus conchae dorsalis, sinus conchae medius, sinus frontalis, sinus maxillaris, sinus lacrimalis, and sinus palatinus. Especially landmarks on these sinuses were stated below.

Concha nasalis dorsalis

In the study, concha nasalis dorsalis was found to extend between front 1/3 part of margo interalveolaris and front 1/3 part of arcus zygomaticus.

Concha nasalis media

Concha nasalis media was found to extend between the mesial of maxillary premolar 2nd tooth and the cervical line of the 3rd maxillary molar tooth.

Concha nasalis ventralis

Concha nasalis ventralis was composed of two convolutions as up and down. It was seen that its front ridge reached the level of posterior part of pulvinus dentalis, and its posterior ridge reached the interproximal level of 2nd and 3rd maxillary molar teeth. It was observed that the cavity between

the alar fold and the basal fold was directly connected with cavum nasi.

Sinus conchae dorsalis

Sinus conchae dorsalis was placed into the concha nasalis dorsalis between the central developmental groove of 1st maxillary premolar tooth and the front level of crista facialis or medial angle of the eye.

Sinus conchae media

It was observed that sinus conchae media placed into concha nasalis media between the cervical line of 2nd maxillary premolar tooth and the mesial surface of the 3rd maxillary molar tooth. It was seen that this sinus was connected with the nasal cavity at the mesial surface of the 3rd maxillary molar tooth.

Sinus frontalis

Sinus frontalis was found to start from the interproximal level between the 3rd maxillary premolar and 1st maxillary molar tooth and extend to the horn base. It was observed that this sinus opened into the meatus ethmoidalis at the level of the mesial cusp of the 1st maxillary molar tooth.

Sinus maxillaris

Sinus maxillaris was found to start from the level of the mesial cusp of 2nd maxillary premolar tooth and extend to the level of lateral angle of the eye. It was detected that the sinus opened into the meatus nasi medius at the level of the 2nd molar tooth. Also, this sinus placed into os zygomaticus.

Sinus lacrimalis

It was detected that the front ridge of sinus lacrimalis rested against the mesial surface of the 1st maxillary molar tooth, and its posterior ridge rested against the medial angle of the eye. It was seen that this sinus was connected with sinus maxillaris at the beginning, and it was connected with meatus nasi medius at the level of the 1st maxillary molar tooth. Also, it was determined that canalis infraorbitalis extended in sinus lacrimalis and sinus maxillaris.

Sinus palatinus

Sinus palatinus was found to extend from the interproximal level of maxillary premolar 1st and 2nd teeth to the distal surface of the 3rd maxillary molar tooth. It was seen that this sinus opened into the aperture maxillopalatina and sinus maxillaris at the level of the 3rd premolar and the 1st molar teeth.

Estimation

The average volumes and surface areas of the sinus paranasales obtained in the study were shown in Table I. According to this information, it was found that the average volume and the surface area of the male Tuj sheep skulls were 76963,89 mm³, and 39595,96 mm² respectively.

Table 1. Volume and surface area values of sinus in Tuj sheep

Parameters	Sinuses	Mean	Minimum	Maximum	SD
Volume (mm ³)	Sinus chonchae dorsalis	1724.15	5315.57	3011.11	1319.69
	Sinus chonchae medius	3048.18	7142.23	4965.3	1605.44
	Sinus frontalis	30686.29	70328.32	49807.08	15719.44
	Sinus lacrimalis	582.43	1482.18	1069.95	365.44
	Sinus maxillaris	10340.24	16715.75	14403.83	2312.09
	Sinus palatinus	2664.15	4258.16	3706.59	584.12
Average		76963.89	49045.44	103721.6	76963.89
Surface area (mm ²)	Sinus chonchae dorsalis	1618.29	3223.08	2367.83	693.23
	Sinus chonchae medius	2257.97	4458.74	3257.6	819.65
	Sinus frontalis	13346.85	29683.25	21027.17	6622.48
	Sinus lacrimalis	711.36	1571.49	1127.76	322.27
	Sinus maxillaris	7094.74	10484.94	8944.95	1283.04
	Sinus palatinus	2331.64	3381.91	2870.62	381.71
Average		39595.96	27360.85	49231.57	39595.95

SD: Standart deviation

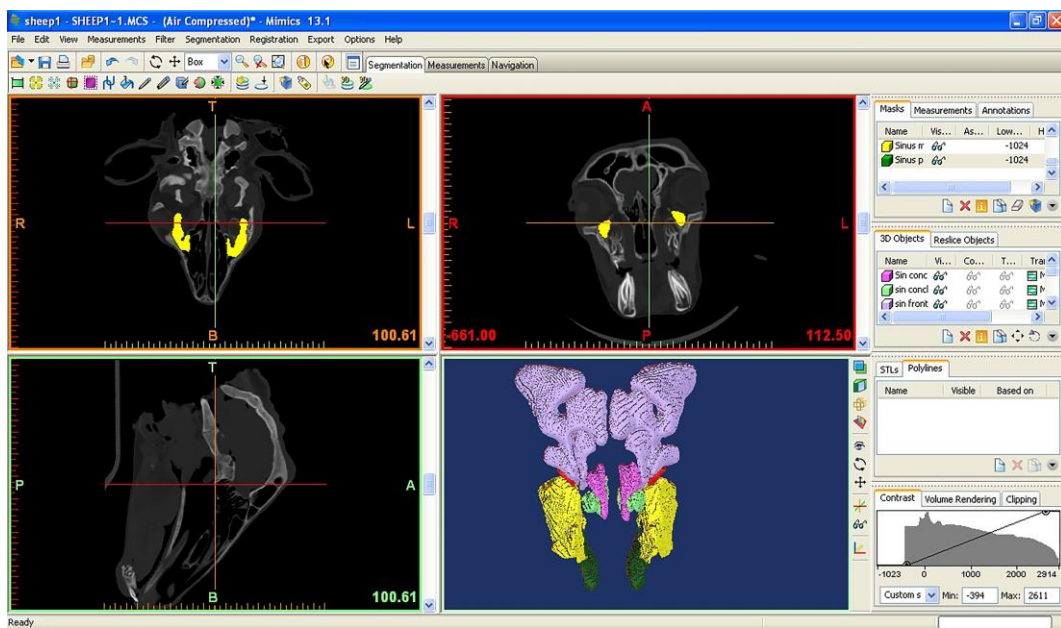


Figure 1. The calculate volume and surface area of sinus paranasales model in Mimics program

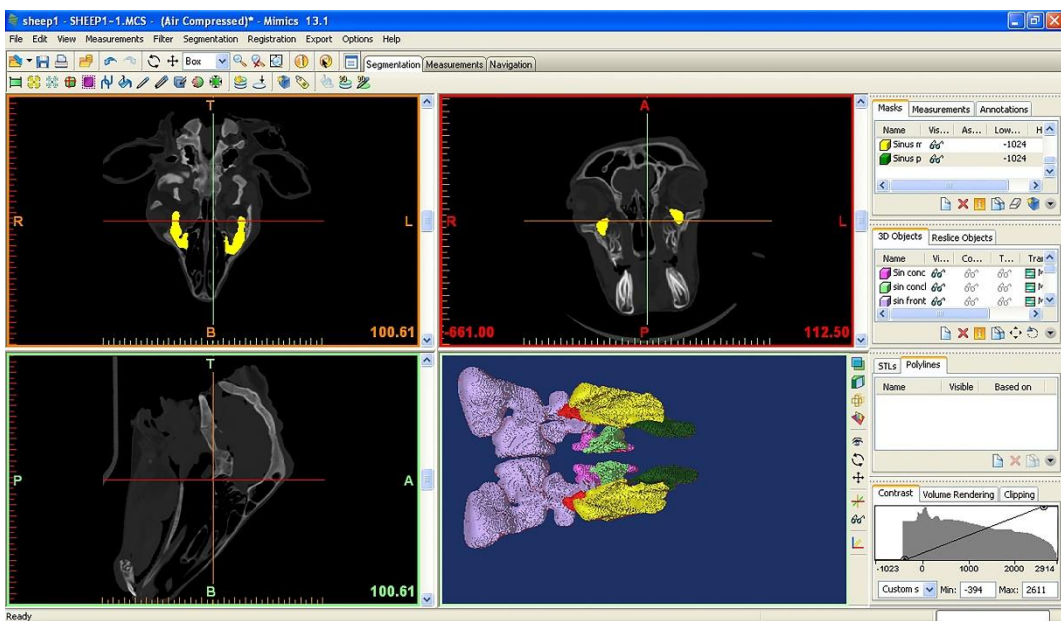


Figure 2. The calculate volume and surface area of sinus paranasales model in Mimics program

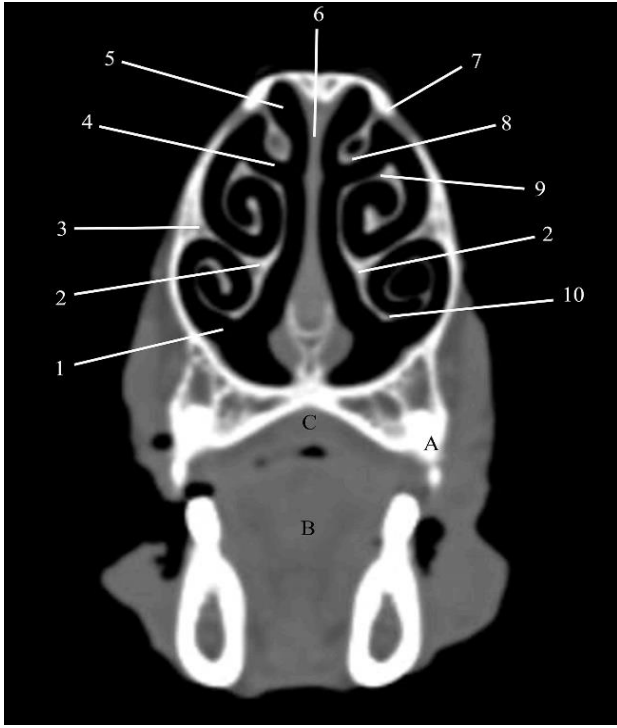


Figure 3. Computed tomography image at the level of 1st upper premolar tooth, A. 1st upper premolar tooth, B. Lingua, C. Palatum durum, 1. Meatus nasi ventralis, 2. Concha nasalis ventralis, 3. Os maxilla, 4. Meatus nasi medius, 5. Meatus nasi dorsalis, 6. Septum nasi, 7. Os nasale, 8. Concha nasalis dorsalis, 9. Dorsal lamina of concha nasalis ventralis 10. Ventral lamina of concha nasalis ventralis

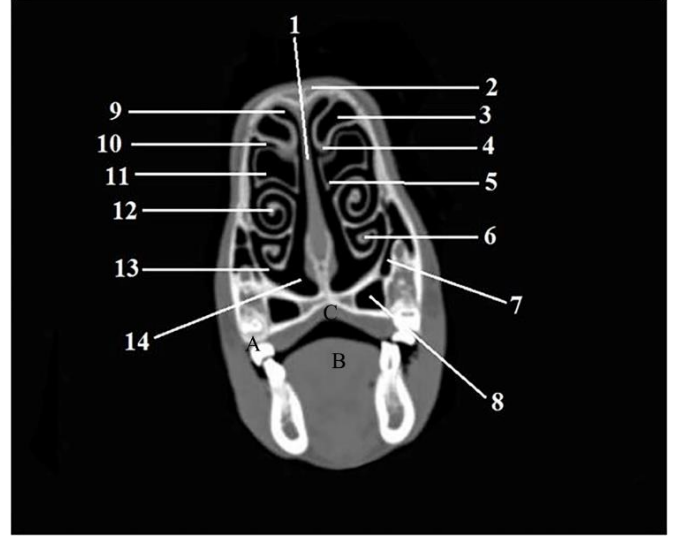


Figure 5. Computed tomography image at the level of 2nd upper premolar tooth, A. 2nd upper premolar tooth, B. Lingua, C. Palatum durum, 1. Septum nasi, 2. Os nasale, 3. Sinus conchae dorsalis, 4. Concha nasalis dorsalis, 5. Concha nasalis medius, 6. Ventral lamina of concha nasalis ventralis, 7. Sinus maxillaris, 8. Sinus palatinus, 9. Meatus nasi dorsalis, 10. Meatus nasi medius, 11. Sinus conchae medius, 12. Dorsal lamina of concha nasalis ventralis, 13. Meatus nasi ventralis, 14. Meatus nasi communis

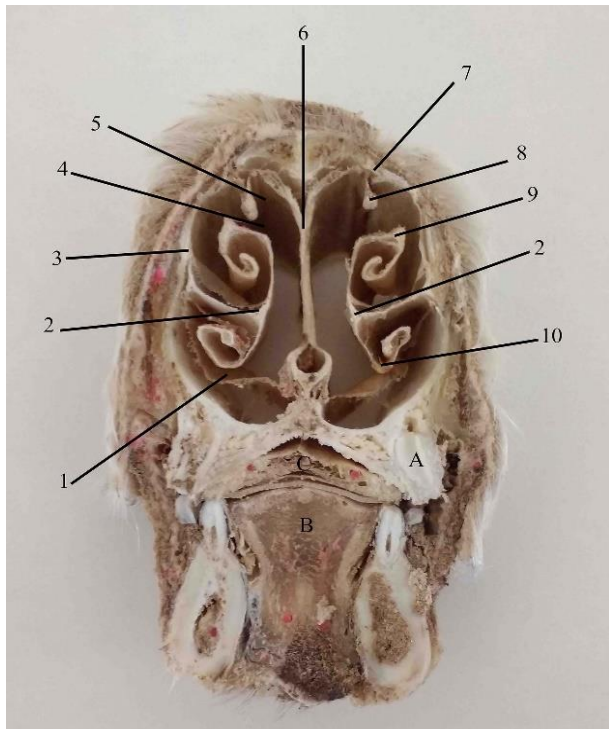


Figure 4. Cross-sectional image at the level of 1st upper premolar tooth, A. 1st upper premolar tooth, B. Lingua, C. Palatum durum, 1. Meatus nasi ventralis, 2. Concha nasalis ventralis, 3. Os maxilla, 4. Meatus nasi medius, 5. Meatus nasi dorsalis, 6. Septum nasi, 7. Os nasale, 8. Concha nasalis dorsalis, 9. Dorsal lamina of concha nasalis ventralis 10. Ventral lamina of concha nasalis ventralis

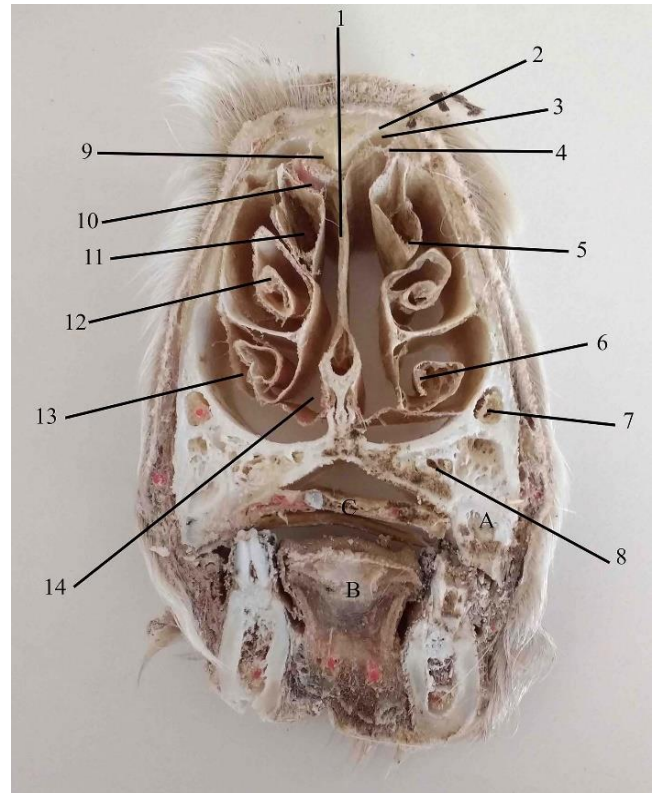


Figure 6. Cross-sectional image at the level of 2nd upper premolar tooth, A. 2nd upper premolar tooth, B. Lingua, C. Palatum durum, 1. Septum nasi, 2. Os nasale, 3. Sinus conchae dorsalis, 4. Concha nasalis dorsalis, 5. Concha nasalis medius, 6. Ventral lamina of concha nasalis ventralis, 7. Sinus maxillaris, 8. Sinus palatinus, 9. Meatus nasi dorsalis, 10. Meatus nasi medius, 11. Sinus conchae medius, 12. Dorsal lamina of concha nasalis ventralis, 13. Meatus nasi ventralis, 14. Meatus nasi communis

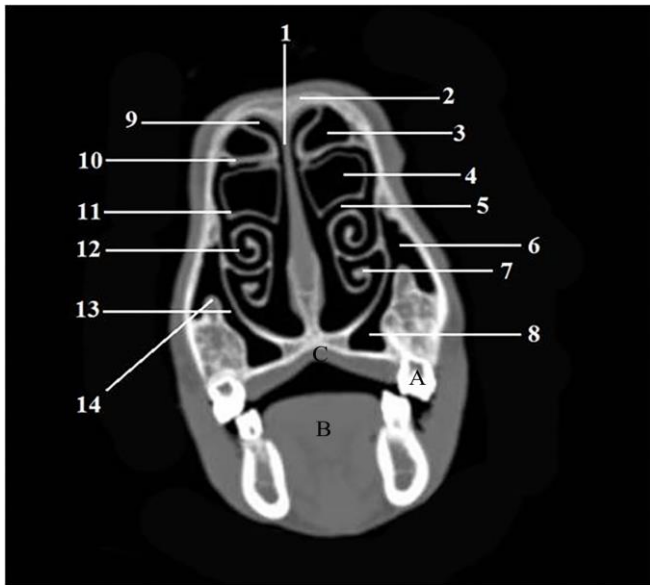


Figure 7. Computed tomography image at the level of 3rd upper premolar tooth, A. 3rd upper premolar tooth, B. Lingua, C. Palatum durum, 1. Septum nasi, 2. Os nasale, 3. Sinus conchae dorsalis, 4. Sinus conchae medius, 5. Meatus nasi medius, 6. Sinus maxillaris, 7. Ventral lamina of concha nasalis ventralis, 8. Sinus palatinus, 9. Meatus nasi dorsalis, 10. Concha nasalis dorsalis, 11. Concha nasalis medius, 12. Dorsal lamina of concha nasalis ventralis, 13. Aditus nasopalatomaxillaris, 14. Canalis infraorbitalis

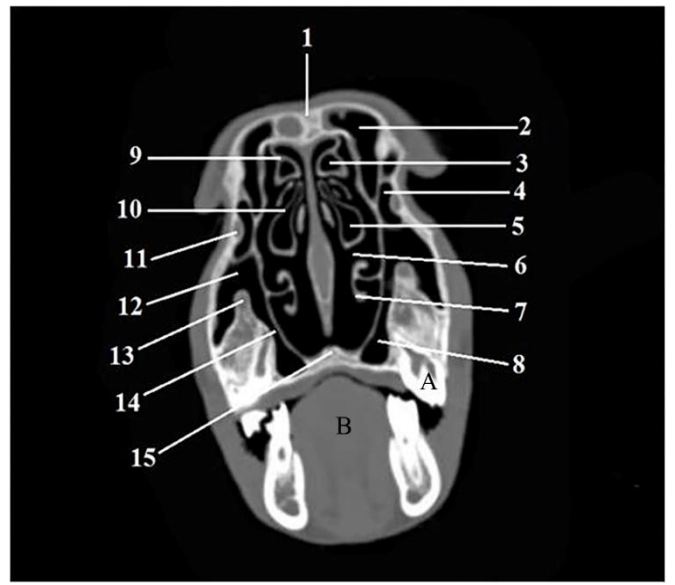


Figure 9. Computed tomography image at the level of 1st upper molar tooth, A. 1st upper molar tooth, B. Lingua, 1. Os frontale, 2. Sinus frontalis, 3. Sinus concha dorsalis, 4. Sinus lacrimalis, 5. Sinus concha medius, 6. Meatus nasi medius, 7. Ventral lamina of concha nasalis ventralis, 8. Sinus palatinus, 9. Concha nasalis dorsalis, 10. Concha nasalis medius, 11. Canalis nasolacrimalis, 12. Sinus maxillaris, 13. Canalis infraorbitalis, 14. Aditus nasopalatomaxillaris, 15. Os vomer

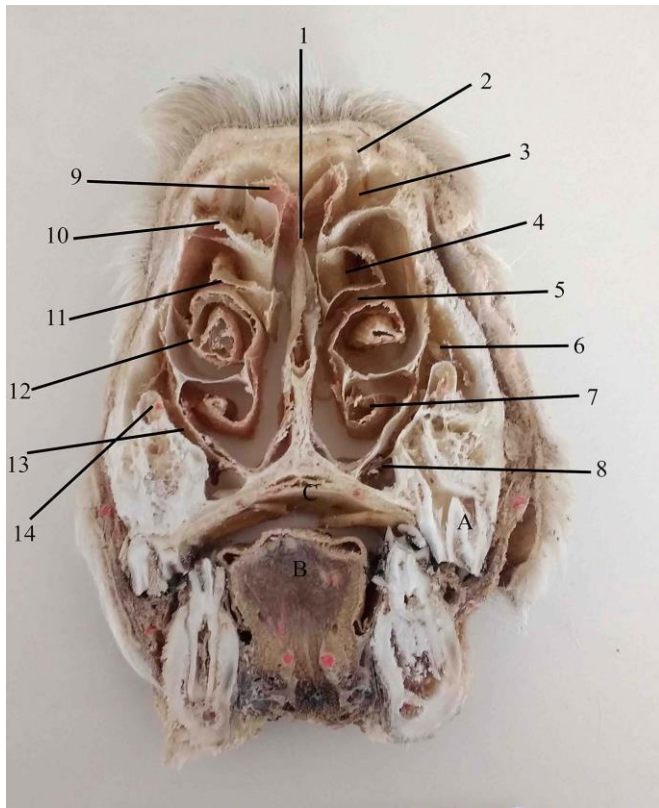


Figure 8. Cross-sectional image at the level of 3rd upper premolar tooth, A. 3rd upper premolar tooth, B. Lingua, C. Palatum durum, 1. Septum nasi, 2. Os nasale, 3. Sinus conchae dorsalis, 4. Sinus conchae medius, 5. Meatus nasi medius, 6. Sinus maxillaris, 7. Ventral lamina of concha nasalis ventralis, 8. Sinus palatinus, 9. Meatus nasi dorsalis, 10. Concha nasalis dorsalis, 11. Concha nasalis medius, 12. Dorsal lamina of concha nasalis ventralis, 13. Aditus nasopalatomaxillaris, 14. Canalis infraorbitalis

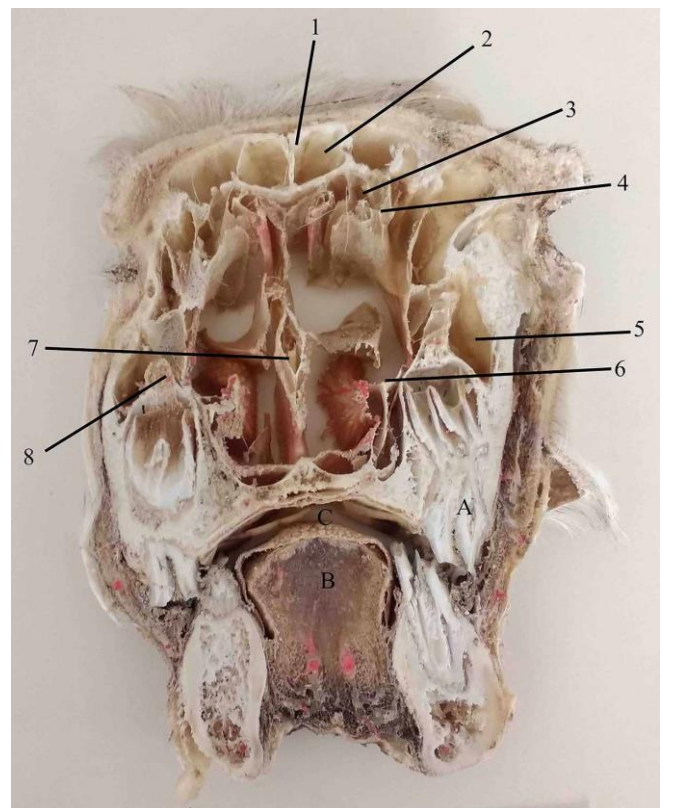


Figure 10. Cross-sectional image at the level of 1st upper molar tooth, A. 1st upper molar tooth, B. Lingua, C. Cavum oris, 1. Septum sinuum frontalis, 2. Sinus frontalis, 3. Sinus concha dorsalis, 4. Concha nasalis dorsalis, 5. Sinus lacrimalis, 6. Concha nasalis ventralis, 7. Septum nasi, 8. Canalis infraorbitalis

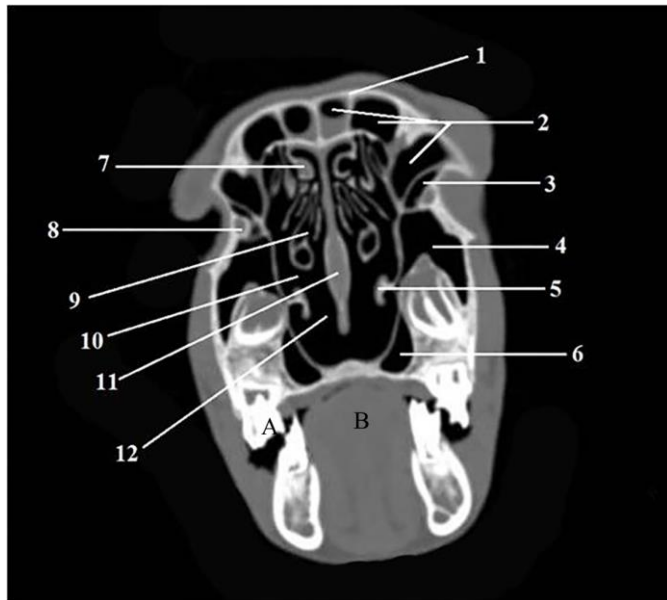


Figure 11. Computed tomography image at the level of 2nd upper molar tooth, A. 2nd upper molar tooth, B. Lingua, 1. Os frontale, 2. Sinus frontalis, 3. Sinus lacrimalis, 4. Sinus maxillaris, 5. Concha nasalis ventralis, 6. Sinus palatinus, 7. Concha nasalis dorsalis, 8. Canalis nasolacrimalis, 9. The section opening to cavum nasi of sinus concha medius, 10. Meatus nasi medius, 11. Septum nasi, 12. Meatus nasi communis

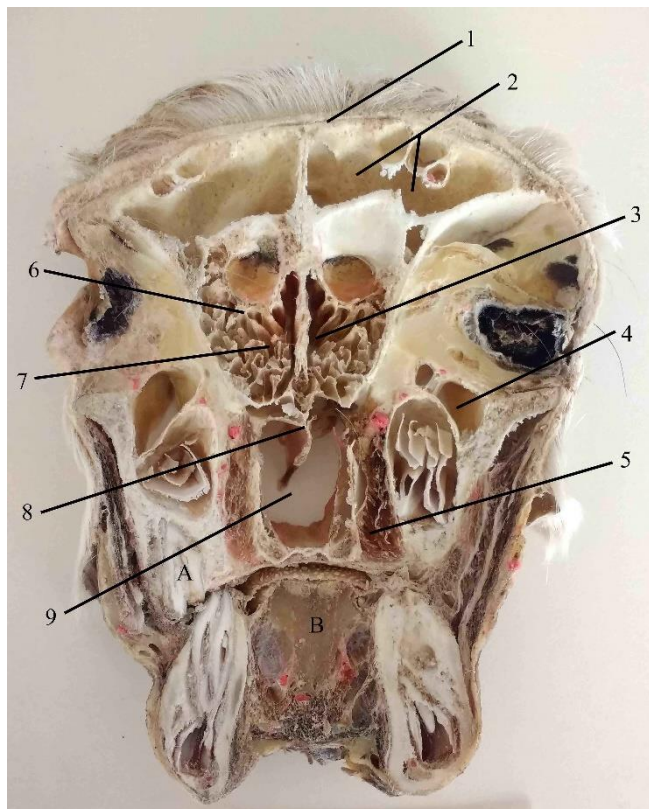


Figure 12. Cross-sectional image at the level of 2nd upper molar tooth, A. 2nd upper molar tooth, B. Lingua, 1. Os frontale, 2. Sinus frontalis, 3. Meatus nasi dorsalis, 4. Sinus maxillaris, 5. Sinus palatinus, 6. Concha nasalis dorsalis, 7. Meatus nasi medius, 8. Septum nasi, 9. Choana

DISCUSSION AND CONCLUSIONS

In veterinary medicine, diagnostic imaging methods (MRI, CT, Ultrasonography, Radiography) are used extensively. It is very important to know how the structures are seen anatomically for detecting the pathological situation. Furthermore, the CT is an alternative imaging method which enables the exploration of structures in the skull region thanks to scanning radiography (8). Regarding that, there are researches (4-9,11,13-19,) in which skull region is scanned with CT in various animal species (horse, dog, cat, goat, and buffalo) in the literature. Unlike these animal species, we described sinus paranasales and related structures of Tuj sheep through transverse section images with computed tomography in the study.

In the study, the skulls of Tuj sheep were displayed with computed tomography at a good resolution and high definition. Cavum nasi, sinus paranasales, and related structures were described on the images clearly. Section images at the level of maxillary premolar and molar teeth were based on while these descriptions were being made. In this part of the study, Alsafy et al. (9), Probst et al. (20) and Shojaei et al. (11) were taken as reference.

Unsalidi (21) told about the existence of sinus sphenoidal in Hasak sheep breed in his study. Nickel et al. (22) stated that sinus sphenoidal and sinus conchae did not exist in small ruminantia. In their study on water buffalos, Alsafy et al. (9) reported that sinus paranasales are maxillary, frontal, palatine, sphenoidal, lacrimal, ethmoidal, dorsal, and median conchal and also he stated that ventral conchal sinus did not exist. In our study, sinus paranasales were found as sinus conchae dorsalis, sinus conchae medius, sinus frontalis, sinus maxillaris, sinus lacrimalis, and sinus palatinus in Tuj sheep. Schaffer and Reed (23) and Farke (24) reported that horn and sinus frontalis extension in it had a function of minimizing the negative effect of extreme power developing from a collision and protecting the brain and the other cranial structures during a fight. In the literature (9,22,25), sinus frontalis was reported to enter the horn with diverticulum cornuale in bovinæ. In our study, the extension of sinus frontalis was observed in processus cornualis in Tuj sheep.

Saigal and Khatra (26) and Alsafy et al. (9) reported that the optimum trepanation point is the midpoint of the distance between margo infraorbitalis and tuber faciale in buffalos. Also, the optimum point for sinus maxillaris trepanation in Tuj sheep supported the literature in our study. Saigal and Khatra (26) stated that the optimum trepanation point for frontal sinus in buffalos is the lateral of the part of the line connecting two temporal regions that coincide with planum medianum. Alsafy et al. (9) stated that cavum cranii extends into the sinus frontalis and they also reported that during trepanation vena frontalis at the level of foramen supraorbitalis might pose a risk. Therefore the researchers (9) described the optimum trepanation point for sinus frontalis in buffalos as the medial of foramen supraorbitalis and vena frontalis, and the line extending through the front edge of the eye. Our research has also concluded that the

optimum trepanation point for sinus frontalis in Tuj sheep is the same as Alsafy et al. (9) stated.

The findings according to the teeth that Sojæi et al. (11) used as a landmark in their study on sinus paranasales and related structures in Rayini goats, and the data obtained in our study were shown comparatively in Table II. According to those data, it was reported in the literature (11) that sinus maxillaris exists at the level of molar teeth (1-3), and sinus palatinus exists at the level of the 3rd premolar with the 1st and the 2nd molar teeth in Rayini goats. Also, Makara (10) reported that sinus palatinus extended from the level of the premolar 2nd and 3rd teeth to the level of the molar 3rd tooth. In our study, it was observed

that sinus maxillaris placed between the 2nd maxillary premolar tooth and lateral angle of the eye when it existed also in os zygomaticus; and it was also observed that sinus palatinus placed at the maxillary premolar 2nd tooth and distal level of the 3rd maxillary molar tooth in Tuj sheep. While Nickel et al. (22) and Getty (27) stated that the sinus maxillaris and the sinus palatinus are connected at the level of the 2nd molar tooth, Sojæi et al. (11) stated that they did not find any connection between the two sinuses in Rayini goats. In our study, it was observed that sinus maxillaris is connected with sinus palatinus with apertura maxillopalatina at the level of the 3rd premolar and the 1st molar teeth.

Table2. Comparative sinus landmarks of Rayini Goat (11) and Tuj Sheep (Study)

Sinuses	Landmarks												
	1st Cheek Tooth		2nd Cheek Tooth		3rd Cheek Tooth		4th Cheek Tooth		5th Cheek Tooth		6th Cheek Tooth		
	Rayini Goat	Tuj Sheep											
Sinus maxillaris	-	-	-	+	-	+	+	+	+	+	+	+	+
Sinus frontalis	-	-	-	-	-	-	-	+	-	+	+	+	+
Sinus palatinus	-	-	-	+	+	+	+	+	+	+	-	-	-
Sinus lacrimalis	-	-	-	-	-	-	-	+	-	+	+	+	+
Sinus conchae dorsalis	-	+	-	+	-	+	-	+	+	+	+	+	-

Makara (10) reported that sinus maxillaris opened into cavum nasi at the level of 4th premolar and 1st molar teeth, and sinus frontalis opened into cavum nasi at the level of 2nd and 3rd molar teeth. In our study, it was observed that sinus maxillaris opened into meatus nasi medius at the level of the 2nd molar tooth, and sinus frontalis opened into meatus ethmoidalis at the level of the 1st molar tooth.

Sinus paranasales in humans (28,29), in primates (30,31), in big ruminantia (32), in rabbits (33), in felidae (34), in rodentia (35), and in equidae (36) were modeled by using the 3D programs. In this study, sinus paranasales in sheep were modeled and their volumes and surface areas were determined for the first time. Bahar et al. (36) stated that the ratio of sinus frontalis and sinus maxillaris to total sinus volume (56.7% and 20.3% respectively) had the highest share, and sinus conchae medius (0.3%) had the lowest share in Arabian foals. In our study, these ratios in sinus frontalis, sinus maxillaris, and sinus conchae medius were found 64.7%, 18.01%, and 6.45% respectively. Besides, different from the literature (36), it was observed that the sinus that had the lowest volume ratio was sinus conchae dorsalis (3.9%).

In rhinology, many animal models such as sheep, rabbit, and pig were tested for the researches (37). In the literature (38) it was suggested that sheep skulls could be used for both training model and practice model in this field. In conclusion, when viewed from this aspect, it is seen that

the data obtained in the study are the first steps for reducing the discussion to breeds and creating new models. For this reason, it is considered that the data and information obtained in this study will enable researchers to make radiological assessments of cavum nasi and sinus paranasales in Tuj sheep, and compare them with the other sheep breeds.

ACKNOWLEDGEMENTS

The permission has been granted from Kafkas University Animal Experiments Local Ethics Committee for the study dated August 31, 2015, with the No.087.

REFERENCES

1. Akcapinar H. (2000). Sheep Farming. 2nd ed., pp: 109-115. Ismat Publishing, Ankara.
2. Ozcan L. (1990). Sheep Farming. Ministry of Agriculture, Forestry, and Rural Affairs, Publication Department, Ankara, 100-103, 113-114.
3. Dursun N. (2000). Veteriner Anatomi II. Medisan Yayınevi, Ankara.
4. Losonsky JM, Abbott LC, Kuriashkin IV. (1997). Computed Tomography of the Normal Feline Nasal Cavity and Paranasal Sinuses. Vet Radiol Ultrasoun. 38(4): 251-258.
5. Morrow KL, Park RD, Spurgeon TL, Stashak TS, Arceneaux B. (2000). Computed Tomographic Imaging of the Equine Head. Vet Radiol Ultrasoun. 41 (6): 491-497.

6. Reetz JA, Mai M, Muravnick KB, Goldschmidt MH, Schwarz T. (2006). Computed Tomographic Evaluation of Anatomic and Pathologic Variations in the Feline Nasal Septum and Paranasal Sinuses. *Vet Radiol Ultrasoun.* 47(4): 321–327.
7. Barrington G, Tucker R. (1996). Use of Computed Tomography to Diagnose Sinusitis in a Goat. *Vet Radiol Ultrasoun.* 37(2): 118–120.
8. Solano M, Brawer RS. (2004). CT of the Equine Head: Technical Considerations, Anatomical Guide, and Selected Diseases. *Clin Tech Equine Pract.* 3(4): 374–388.
9. Alsafy MAM, El-Gendy SAA, El Sharaby AA. (2013). Anatomic Reference for Computed Tomography of Paranasal Sinuses and Their Communication in the Egyptian Buffalo (*Bubalus bubalis*). *Anat Histol Embryol.* 42(3): 220-31.
10. Makara M. (2010). Computed Tomography, Cross Sectional Anatomy and Measurements in the Head of Normal Goats, PhD Thesis, University of Zurich, Switzerland.
11. Shojaei B, Nazem MN, Vosough D. (2008). Anatomic Reference for Computed Tomography of the Paranasal Sinuses and Their Openings in the Rayini Goat. *Iran J Vet Surg.* 3(2): 77–85.
12. International Committee on Veterinary Gross Anatomical Nomenclature. (2017). General Assembly of the World Association on Veterinary Anatomists. *Nomina Anatomica Veterinaria.* 6th edition. Gent, Belgium.
13. Arencibia A, Vazquez JM, Ramirez-Gonzalez JA, et al. (1997). Anatomy of the Craniocervical Structures of the Goat (*Capra hircus* L.) by Imaging Techniques: A Computerized Tomographic Study. *Anat Histol Embryol.* 26(3): 161–164.
14. De Zani D, Borgonovo S, Biggi M, et al. (2010). Topographic Comparative Study of Paranasal Sinuses in Adult Horses by Computed Tomography, Sinuscopy, and Sectional Anatomy. *Vet Res Commun.* 34(Suppl. 1): 13-16.
15. El-Gendy SA, Alsafy MAM. (2010). Nasal and Paranasal Sinuses of the Donkey: Gross Anatomy and Computed Tomography. *J Vet Anat.* 3(1): 25–41.
16. Koch R, Schroder H, Waibl H. (2002). Topography and Imaging Methods (X-rays and Computer Tomography) on the Paranasal Sinuses of Cats. *Kleintierpraxis.* 47, 213–219.
17. Kraft SL, Gavin P. (2001). Physical Principles and Technical Considerations for Equine Computed Tomography and Magnetic Resonance Imaging. *Vet Clin North Am Equine Pract.* 17: 115–130.
18. Smallwood JE, Brett C, Wood BC, Taylor WE, Lloyd P. (2002). Anatomic Reference for Computed Tomography of the Head of the Foal. *Vet Radiol Ultrasoun.* 43(2): 99–117.
19. Tucker RL, Farrell E. (2001). Computed Tomography and Magnetic Resonance Imaging of the Equine Head. *Vet Clin North Am Equine Pract.* 17(1): 131–144.
20. Probst A, Henninger W, Willmann M. (2005) Communications of Normal Nasal and Paranasal Cavities in Computed Tomography of Horses. *Vet Radiol Ultrasoun.* 46(1), 44–48.
21. Unsaldi E. (2012). Hasak Melez Koyun Tipinde Neurocranium'un Makroanatomik İncelenmesi. *Firat Üni Sag Bil Derg.* 26 (1): 01 – 07
22. Nickel R, Schummer A, Seiferle E. (1986). The Anatomy of the Domestic Animals. Volume I. The Locomotor System of Domestic Mammals. Translation from the 5th German edition. Page: 137–139; 157–158. Verlag Paul Parey, Berlin. Hamburg.
23. Schaffer WM, Reed CA. (1972). The Co-evolution of Social Behavior and Cranial Morphology in Sheep and Goats (*Bovidae*, *Caprini*). *Fieldiana.* 61, 1–88.
24. Farke AA. (2008). Function and Evolution of the Cranial Sinuses in Bovid Mammals and Ceratopsian Dinosaurs. PhD thesis in anatomical sciences, Stony Brook University.
25. Budras KD, Habel RE (2003). *Bovine Anatomy, An Illustrated Text*, 1st ed. Schlutersche GmbH & Co. KG. Page: 34–35. Verlag und Druckerei. Hannover.
26. Saigal RP, Khatra GS. (1977). Paranasal Sinuses of the Adult Buffalo (*Bubalus bubalis*). *Ann Anat.* 1977: 141(1): 6–18.
27. Getty R. (1975). *Sisson and Grossman's the Anatomy of the Domestic Animals.* Vol. 1. 5th Ed. Page: 785-786. WB Saunders Co, Philadelphia.
28. Kawarai Y, Fukushima K, Ogawa T, et al. (1999). Volume Quantification of Healthy Paranasal Cavity by Three-dimensional CT Imaging. *Acta Otolaryngol.* 540(Suppl.): 45–49.
29. Pirner S, Tingelhoff K, Wagner I, et al. (2009). CT-based Manual Segmentation and Evaluation of Paranasal Sinuses. *Eur Arch Oto rhinolaryngol.* 266(4): 507–518.
30. Nishimura TD, Takai M, Tsubamoto T, Egi N, Shigehara N. (2005). Variation in Maxillary Sinus Anatomy Among Platyrrhine Monkeys. *J Hum Evol.* 49(3): 370–389.
31. Rae TC, Koppe T. (2000). Isometric Scaling of Maxillary Sinus Volume in Hominoids. *J Hum Evol.* 38(3): 411–423
32. Farke AA. (2010). Evolution and Functional Morphology of the Frontal Sinuses in Bovidae (Mammalia: Artiodactyla), and Implications for the Evolution of Cranial Pneumaticity. *Zool J Linn Soc.* 159(4): 988–1014.
33. Casteleyn C, Cornillie P, Hermens A, et al. (2010). Topography of the Rabbit Paranasal Sinuses as a Prerequisite to Model Human Sinusitis. *Rhinology.* 48(3): 300–304.
34. Siliceo G, Salesa MJ, Anton M, Pastor JF, Morales J. (2011). Comparative Anatomy of the Frontal Sinuses in the Primitive Sabre-toothed felid *Promegantereon Ogygia* (Felidae, Machairodontinae) and Similarly Sized Extant Felines. *Estud Geol-Madrid.* 67(2): 277–290.
35. Phillips JE, Ji L, Rivelli MA, Chapman RW, Corboz MR. (2009). Three-dimensional Analysis of Rodent Paranasal Sinus Cavities from X-ray Computed Tomography (CT) Scans. *Can J Vet Res.* 73(3): 205–211.
36. Bahar S, Bolat D, Dayan MO, Paksoy Y. (2014). Two- and Three-dimensional Anatomy of Paranasal Sinuses in Arabian foals. *J Vet Med Sci.* 76(1): 37–44.
37. Li PM, Downie D, Hwang PH. (2009). Controlled steroid delivery via bioabsorbable stent: safety and performance in a rabbit model. *Am J Rhinol Allergy.* 23(6): 591-596.
38. Awad Z, Touska P, Arora A, Ziprin P, Darzi A, Tolley NS. (2014). Face and Content Validity of Sheep Heads in Endoscopic Rhinology Training. *Int Forum Allergy Rhinol.* 4(10):851-858.

✉ **Corresponding author:**

Yasin DEMIRASLAN

Department of Anatomy Faculty of Veterinary Medicine

Mehmet Akif Ersoy University, Burdur-15100- TURKEY

E-mail: yasindemiraslan@hotmail.com